Exterior Decay of Wood–Plastic Composite Boards: Characterization and Magnetic Resonance Imaging

Rebecca Ibach Grace Sun Marek Gnatowski Jessie Glaeser
Mathew Leung John Haight

Abstract

Magnetic resonance imaging (MRI) was used to evaluate free water content and distribution in wood–plastic composite (WPC) materials decayed during exterior exposure because moisture is an essential factor for the progression of the decay process. Two segments of the same board were selected from six commercial decking boards that showed signs of decay (from a total of 27 boards that were exposed near Hilo, Hawaii). The decay process was indicated by the presence of fungal fruiting bodies. One of the two board segments was exposed in sun, the other in shadow. Whole board segments were imaged using a clinical MRI unit, and then selected areas were examined using scanning electron microscopy (SEM). Samples were cut from the cross section of the board to determine material density as an indicator of the degree of decay advancement. The presence of free water detected by MRI was correlated to the mechanism of decay in the WPC board segments and to the water distribution measured in the boards. Both board segments showed a significant amount of decay, where SEM images showed the presence of fungal hyphae inside the boards, particularly the segment exposed in shadow. MRI showed that the expected pattern of free water distribution—a moisture gradient from greatest on the outside of the board to least inside—was not evident in the decayed board evaluated in this study. On the contrary, a reverse moisture gradient was observed in some areas where there appeared to be a relatively high concentration of free water in the center of the board. This could be explained by moisture transfer of fungal mycelia into the core of the board and the generation of water as decay fungi metabolize wood.

Wood–plastic composites (WPCs) are a relatively recent generation of materials in which wood is used as a filler or for reinforcement; they are used for many exterior and interior applications (Hanawalt 2012). A large portion (about two-thirds) is utilized for outdoor construction, such as decking, railings, and fencing, and for exterior cover applications, such as siding and trim. These new WPC products are designed for long-term performance, consistent appearance, and dimensional stability (Smith and Wolcott 2006). These materials were initially considered to be very resistant to decay because of slow moisture transport into the material achieved by at least partial encapsulation of the wood particles by the polymer matrix (Naghipour 1996). Such findings were contradicted by observations of fungal decay fruiting bodies on WPC boards along walkways in the Everglades in Florida (Morris and Cooper 1998), which stimulated research on the decay of such materials, which are usually 50 to 60 percent wood by weight.

Early laboratory and field studies indicated that the wood component in WPC could be susceptible to decay (Morris and Cooper 1998; Laks and Verhey 2000; Mankowski and Morrell 2000; Verhey et al. 2001, 2003; Clemons and Ibach 2002; Ibach and Clemons 2002; Pendleton et al. 2002; Laks et al. 2010; Ibach et al. 2013). Fungal decay fruiting bodies that appear on WPCs have been described (Morris and Cooper 1998, Manning and Ascherl 2007, Laks et al. 2010), but the mechanism of this process and extent of growth of fungal hyphae within the mixture of wood and plastic is not known. Particularly intriguing is the process of destruction

The authors are, respectively, Research Chemist, USDA Forest Serv. Forest Products Lab., Madison, Wisconsin (ribach@fs.fed.us [corresponding author]); Materials Researcher and Research Director, Polymer Engineering Co., Ltd., Burnaby, British Columbia, Canada (grace.sun@polymerengineering.ca, mgnatowski@polymerengineering.ca); Research Plant Pathologist, USDA Forest Serv. Northern Research Station, Center for Forest Mycology Research, Newton Square, Pennsylvania (jglaeser@fs.fed.us); Research Scientist, Polymer Engineering Co. Ltd., Burnaby, British Columbia, Canada (mleung@polymerengineering.ca); and Biological Laboratory Technician, USDA Forest Serv. Northern Research Station, Center for Forest Mycology Research, Newton Square, Pennsylvania (jhaight@fs.fed.us). This article was received for publication in March 2015. Article no. 15-00011.

Forest Prod. J. 66(1/2):4–17.
doi:10.13073/FPJ-D-15-00011

by decay fungi of some WPC commercial products exposed to fluctuations in moisture, temperature, and ultraviolet radiation in outdoor applications. It was recently found during testing of some decayed WPCs that aggressive attack by decay fungi may be preceded by a prolonged period of time, or an initiation period, with no visible signs of fungal activity (Ibach et al. 2013). On the other hand, in another study where samples of selected types of commercial WPCs were exposed for 10 years in Hilo, Hawaii, samples were found where degradation was mainly limited to shallow areas near the surface, and the presence of wood decay fungi was not detected (Schauwecker et al. 2006).

In the WPC wood component, a moisture content (MC) of greater than 25 percent is required to support fungal growth, which may be accelerated by elevated temperature (Ibach et al. 2004; Lopez et al. 2005; Shirp and Wolcott 2005; Manning and Ascherl 2007; Kim et al. 2008, 2009; Lomelí-Ramírez et al. 2009; Defoirdt et al. 2010; Fabiyi et al. 2011; Segerholm et al. 2012). The decay process damages the wood component (e.g., cellulose and lignin) of WPC, leaving behind cavities or voids. Mycelia of decay fungi can frequently be observed as a part of this process (Mankowski and Morrell 2000, Ibach et al. 2013).

Magnetic resonance imaging (MRI) is a well-established method for imaging mobile water in wood, with the first work in this field published over 25 years ago (Hall et al. 1986, Wang and Chang 1986), though bound water and other protons present in wood or a synthetic polymer structure are not visible during MRI experiments (MacMillan et al. 2011). Detailed reviews of literature in the field of application of magnetic resonance for wood-related research were prepared by Bucur (2003) and more recently by Stenstrom et al. (2009). MRI was found to be a versatile application in wood science. Olson and Chang (1990) applied MRI to measure MC and moisture distribution in wood during the drying process. A specially designed portable MRI system was used in the forest for in situ analysis of living trees (Jones et al. 2012). MRI was also used for the evaluation of thermally modified wood (Telkki et al. 2010). Plants other than wood, for example broccoli, were also imaged using an MRI system to find moisture distribution during the drying process (Jin et al. 2011).

MRI can also be used for early detection of fungal decay in wood based on findings of increased MC (Müller et al. 2001). To metabolize wood, decay fungi require a high MC, usually above the fiber saturation point, but they also generate a significant amount of water as a result of the wood degradation process by this known reaction:

$$C_6H_{12}O_6 + 6O_2 = 6CO_2 + 6H_2O$$

Degraded wood thus releases bound water, which increases the MC of the remaining wood component (Kirk and Cowling 1984). By obtaining MRI images at two different stages of fungal activity, Müller et al. (2001) were able to determine that the decay process did in fact increase the MC of the wood, particularly in localized areas adjacent to fungal hyphae, and that this increase could be detected by this imaging method.

We have recently demonstrated the use of a clinical MRI for imaging free water above the fiber saturation point in WPC boards exposed in exterior conditions in Vancouver, British Columbia, and Hilo, Hawaii (Gnatowski et al. 2014). It was found that free water accumulates exclusively in the exterior portion of the extrudates and particularly in board support areas, along the ''drip edge'' on the back side of the board, and in the vicinity of the exposed board surface and its edges. Figure 1 shows a cross-sectional schematic of the typical moisture distribution in a WPC board exposed to exterior conditions, as seen in MRI images.

In this article, we demonstrate the use of MRI as a novel, nondestructive method to examine moisture concentration and distribution above wood fiber saturation point within an exterior-exposed commercial decking board showing signs of fungal decay activity. The MRI technique provides a relatively detailed, nondestructive, three-dimensional glimpse into the decay process in WPCs.

Materials and Methods

Chemicals (decahydronaphthalene, 2.2 methylenebis (6-tert-butyl-4-methylphenol, isopropyl alcohol, acetone) were obtained from Aldrich Chemical Company (Milwaukee, Wisconsin).

Exposure, inspection, and collection of boards

Twenty-seven randomly selected commercial decking boards, made by seven different manufacturers, were purchased from a building materials outlet. Each board was cut into three segments, one reference and two exterior exposures. These segments will be henceforth referred to as boards for simplification purposes. The reference board was used for characterization of the material, including density, water absorption (WA) of the WPC, MC in the wood, and wood content, particle size, and distribution. The thermoplastic resin used in the extrusion of the board was also characterized. The two other boards were exposed outside near Hilo, Hawaii, from November 2004 to November 2012. One of the boards was mainly exposed in semishadow under an Albizia tree for most of its exposure (shadow), while the second board was exposed in an open area under full sunlight (sun). Boards were periodically inspected and tested. Six boards (from a total of 27 boards) showed signs of decay. After 8 years of exposure, one set of boards (sun and shadow) that showed early decay symptoms in the form of fungal fruiting bodies was selected for this study.

Shadow and sun boards were exposed in a horizontal position and fastened with two screws to a frame made from treated wood. The boards were installed about 914 mm (36 in.) above the ground. Hilo has an average annual precipitation of 3,200 mm (126 in.) and average daytime annual temperatures with highs around 27.2°C (80.9°F) and lows around 19.3°C (66.8°F). Boards at both sun and shadow sites were periodically inspected and their condi-

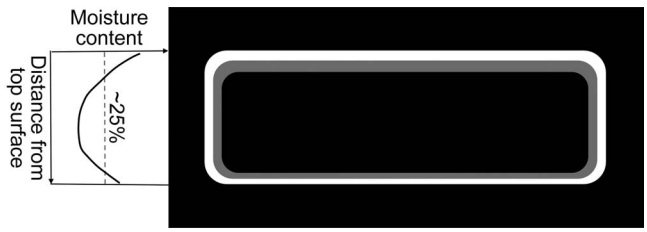

Figure 1.—Cross-sectional schematic of the typical moisture distribution in a wood–plastic composite board exposed to exterior conditions as seen in magnetic resonance images, with the light area indicating presence of free water.

tions documented, and sections of the boards were collected for evaluation of MC and distribution. In November 2012, collected sections were wrapped in several layers of plastic wrap film, placed inside a polystyrene foam insulated box, and couriered overnight to the laboratory. The board sections remained wrapped and stored at around 15°C until MRI was conducted 2 days after their arrival. The lengths of these sections were 59 and 61 cm (23 and 24 in.) for the shadow and sun boards, respectively.

Fungal identification

Fungal fruiting bodies were removed from the WPC boards and dried at 50°C to prevent additional fungal growth. The fruiting bodies were examined by light microscopy at 1,000× using Melzer's reagent and KOH/0.5 percent safranin on an Olympus BX40 microscope and identified using keys and descriptions from Hemmes and Desjardin (2002) and Gilbertson and Ryvarden (1986, 1987).

Density and WA

The density and WA of the reference board were measured according to ASTM standards D1037 and D7031 (ASTM International 2014a, 2014b). The original board surfaces were maintained. The ovendried density was measured using six rectangular samples obtained across the width of the board, with nominal dimensions 38 by 8.4 by 10 mm (1.5 by 0.3 by 0.4 in.). A WA sample with dimensions 38 by 140 by 152 mm (1.5 by 5.5 by 1.5 in.) was conditioned for 2 days at 20°C and 65 percent relatively humidity prior to immersion in distilled water maintained at the same temperature. After 24 hours of water immersion, the sample was dried in an oven at 103°C for 2 days. WA of the sample and corresponding MC based on the wood content were determined with respect to total water uptake from storage of the board and after 24 hours of water immersion. The WA and MC properties of the board were compared with those of a solid wood board of Bigleaf maple (*Acer macrophyllum*) and to a rectangular-shaped segment of polyethylene plastic with dimensions similar to the WPCs, both tested in a similar manner.

The densities of the field-exposed sun and shadow boards were also determined using the same procedure and sample sizes as described above. Similar to the reference board, six rectangular samples from each of the sun and shadow locations were obtained across the width of the board sample collected in 2012. Only four samples collected in 2009 were used because of the limited availability of material, which was also used for destructive evaluation of water absorption and distribution inside the boards.

WPC characterization

The reference board was characterized based on procedures used and described by the authors in a previous publication (Gnatowski et al. 2014). Wood content was analyzed by dissolving a sample of the ovendried composite in decahydronaphthalene solution. Additionally, approximately 1 g of WPC sample was ashed at 675°C and 900°C to find the quantity of inorganic pigments and fillers present. Resins used in manufacturing of the composite were characterized based on Fourier transform infrared (FTIR) spectra and differential scanning calorimetry (DSC) thermograms. Wood flour particles from the commercial board were recovered after dissolving polyethylene from the WPC material and were characterized by optical microscopy with respect to their aspect ratio, size, and size distribution.

Destructive testing for WA and MC distribution

Samples from the shadow and sun boards collected after different exposure periods were cut into thin wafers using a bandsaw with a target nominal thickness of 1 mm (0.039 in.) to measure WA and MC distribution (Ibach et al. 2013, Gnatowski et al. 2014). WA and MC distributions at a distance from the cut edge or through the thickness of the board were determined by wafering and drying wafers at 103°C. MC was calculated based on known wood content. Results are presented in terms of calculated MC as a function of normalized distance from the board's surface.

Scanning electron microscopy

To determine decay characteristics associated with the different levels of ovendried densities recorded, two areas each from the sun and shadow boards collected in 2012 were sampled for scanning electron microscopy (SEM). Rectangular pieces 0.5 by 0.5 by 1 cm were cut from the center of each board sample using double-edged razor blades and then dried overnight in a desiccator. Samples were next mounted on stubs, sputter-coated with gold for 6 minutes in a Denton Desk 1 vacuum evaporator (Denton Vacuum, Moorestown, New Jersey), and examined using a Leo Evo 40 electron microscope (Carl Zeiss, NTS, Peabody, Massachusetts).

Magnetic resonance imaging

MRI of the boards was carried out by the Canadian Magnetic Imaging Laboratory in Vancouver, British Columbia, using a clinical Siemens Magnetom Espree 1.5 Tesla model TIM [32 by 8] MRI system (Siemens, Germany). This instrument provided an image zone with

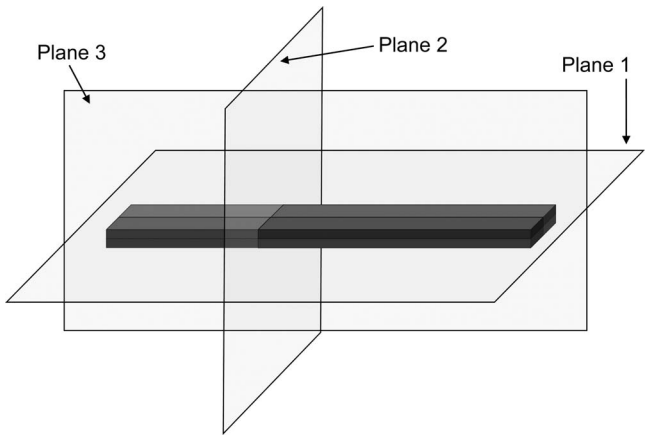

Figure 2.—Schematic orientation of magnetic resonance imaging planes on the wood–plastic composite boards. Plane 1, 4-mm slice in the horizontal plane; Plane 2, 8-mm slice in vertical plane perpendicular to the board length; Plane 3, 8-mm slice in a vertical plane parallel to the board length.

Table 1.—Characterization of solid wood, the reference board, and polyethylene.

Material	Wood content (%)	Density (g/cm^3)[a]	Total water uptake from storage (%)[b,c]		Total water uptake from storage and 24-h water immersion (%)[b,c]		Water absorption from 24-h water immersion only (%)[b]
			Water absorption	Moisture content	Water absorption	Moisture content	Overall
Solid wood[d]	100	0.45	11.01	11.01	31.84	31.84	20.83
Reference	52.9	0.92	0.93	1.76	2.47	4.67	1.54
Polyethylene	0	0.92	0.00	NA[e]	0.02	NA	0.02

[a] Measured using ovendried samples (103°C for 2 days).
[b] Determined as per ASTM D7031 and D1037 (ASTM International 2014a, 2014b).
[c] Water absorption is the water mass in the wood–plastic composite sample while moisture content is calculated as the water mass divided by the wood content.
[d] Western maple.
[e] NA = not applicable.

field of view 320 mm (12.6 in.) along the WPC board length. The image matrix 521 by 521 corresponded to the spatial resolution of about 0.55 by 0.55 mm. For image acquisition, flash gradient echo sequence was used with an echo time of 2.7 ms and repetition time of 6.1 ms. MRI scans of the entire boards were conducted in three planes shown in Figure 2. The majority of the scans were performed using the following slicing thickness: Plane 1, 4-mm slicing in a horizontal plane; Plane 2, 8-mm slicing in a vertical plane perpendicular to board length; and Plane 3, 8-mm slicing in a vertical plane parallel to the board length. This selection of slice thickness combined sufficient image detail quality with reasonable imaging time. For both shadow and sun boards, 10 slices were imaged in Plane 1 and 18 slices were imaged in Plane 3. With respect to Plane 2, 74 and 80 slices were imaged for the shadow and sun boards, respectively. It was expected that only free water above the fiber saturation point in the wood, which was the primary interest, would be visible on the image in the form of brighter areas owing to the relatively long signal lifetime of mobile or free water. Only selected images are presented in this article.

Results and Discussion

Characterization of the reference board segment

Table 1 shows WA and MC of the WPC boards with respect to their total water uptake from storage and 24 hours of water immersion. Results for maple solid wood and polyethylene, at identical test conditions, are also presented in Table 1. The density of the reference board was 0.92 g/cm^3.

Quantitative extraction of a portion of the reference board yielded a wood flour content of 53 percent. The extracted

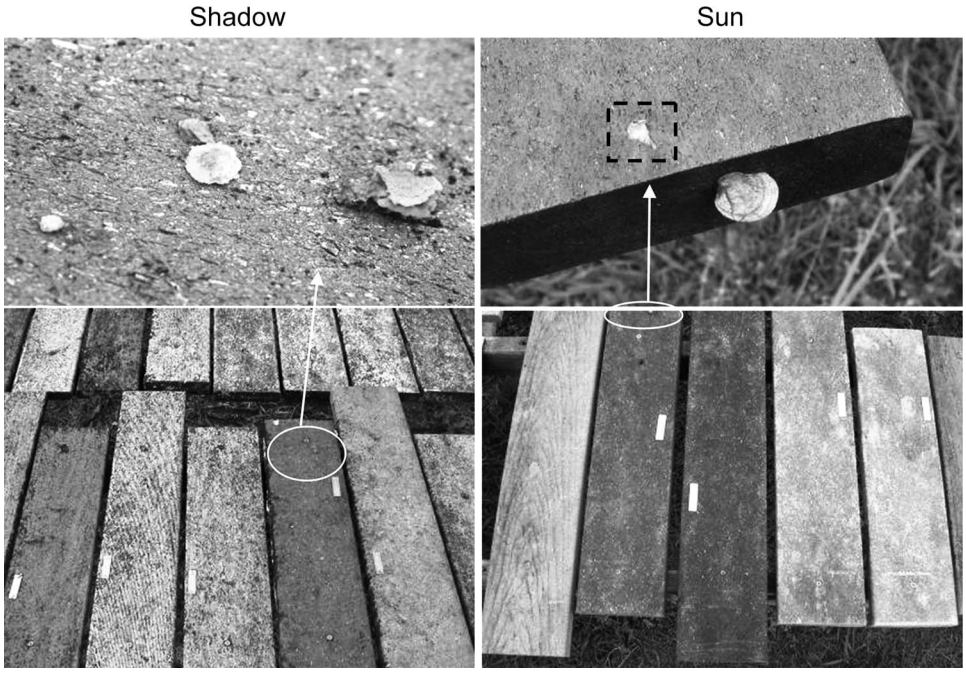

Figure 3.—Shadow (left) and sun (right) boards exposed at their respective locations in 2009, after 51 months of exposure. Areas of interest containing fungi fruiting bodies are marked with circular annotations; an example of a composite defect is enclosed in the dotted lines.

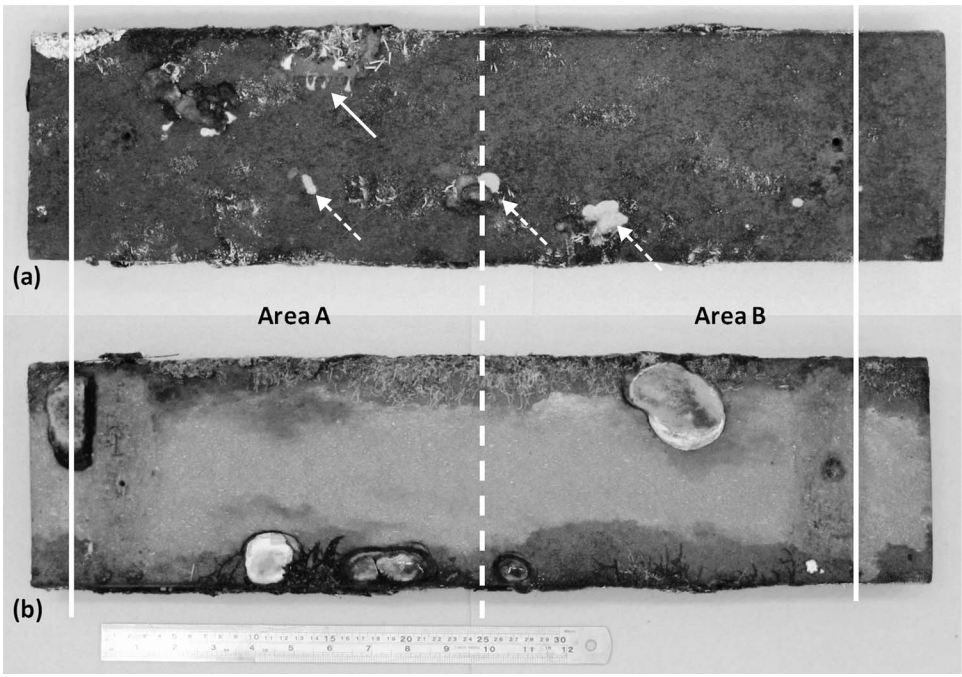

Figure 4.—Shadow board (a) top (exposed) side and (b) bottom side after 51 months of exposure, where the dotted line shows the division between areas A and B, which were imaged separately due to the limitation of the magnetic resonance imaging equipment. The arrow with the solid line points to Dacryopinax spathularia, *a jelly fungus that causes brown-rot; the arrows with dashed lines point to fruiting bodies of a polypore, tentatively identified as* Pycnoporus sanguineus, *a white-rot fungus*.

matrix was precipitated, filtered, washed, dried, and then analyzed by FTIR, yielding a spectrum showing characteristic peaks for polyethylene. Additionally, analysis by DSC showed resin melting temperature peaks of 112°C and 125°C, establishing that the polyethylene was most likely a blend of low-density and linear low-density resins.

The wood flour particles used in the reference board had an average particle surface area of 0.046 mm^2. The average aspect ratio of the wood flour particles was measured as 3.39, which is in good agreement with data from literature (Klyosov 2007). Ash content of the board was 1.9 percent at both 675°C and 900°C, which was most likely associated

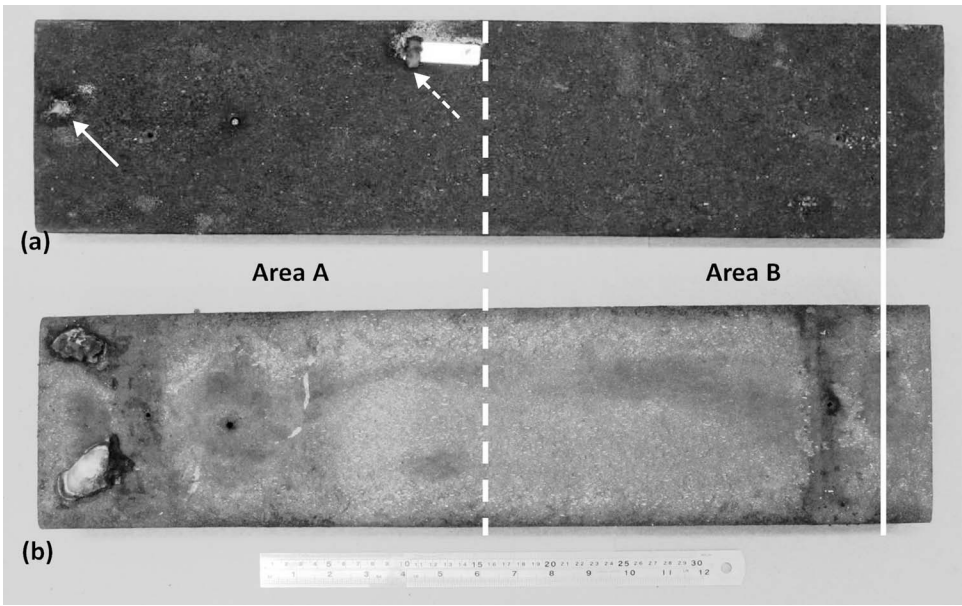

Figure 5.—Sun board (a) top (exposed) side and (b) bottom side after 51 months of exposure, where the dotted line shows the division between areas A and B, which were imaged separately due to the limitation of the magnetic resonance imaging equipment. The arrow with a dashed line points to fruiting bodies of a polypore, tentatively identified as Pycnoporus sanguineus, *a white-rot fungus; the arrow with a solid line points to fruiting bodies of* Chlorociboria *sp., a stain fungus*.

Table 2.—Density measurements of the reference, shadow, and sun boards collected in different years.[a]

Sample type	Collection year	Density at various locations (g/cm^3)						Avg. (SD) density (g/cm^3)
		1	2	3	4	5	6	
Reference	NA	0.91	0.93	0.93	0.93	0.92	0.92	0.92 (0.01)
Shadow	2009	0.91	0.92	—	—	0.92	0.91	0.92 (0.01)
Sun	2009	0.92	0.93	—	—	0.92	0.90	0.92 (0.01)
Shadow	2012	0.68	0.73	0.66	0.60	0.60	0.62	0.65 (0.05)
Sun	2012	0.89	0.91	0.89	0.81	0.67	0.65	0.80 (0.12)

[a] NA = not applicable; — = data were not available due to the limitations of the specimens sampled.

with small quantities of wood inorganic compounds and pigment added by the manufacturer.

Inspections of the WPC boards

After 28 months of field exposure (in 2007), the shadow and sun boards showed no obvious signs of fungal growth. However, periodic field inspections after 40 months showed a single fruiting body of a decay fungus on the board at the sun location. Further inspection a year later showed several fruiting bodies on boards exposed in both sun and shadow locations. Additional fruiting bodies were observed with increasing exposure time. Figure 3 shows the shadow and sun boards in 2009 (51 mo of exposure) with visible fruiting bodies. This was the last inspection of the boards before their collection for evaluation in 2012. Some of the fruiting bodies visible on the surface of the boards after 8 years of exposure (November 2012) were photographed just before the detailed examinations described in this article (Figs. 4 and 5). The boards maintained their integrity, and wood particles were still visible in the cross sections despite the extensive decay detected from the density loss between reference and exposed samples, as described in the next section.

At least six different species of wood-inhabiting fungi were fruiting on the boards. The bright yellow fruiting bodies (Fig. 4a) are *Dacryopinax spathularia,* a jelly fungus that causes brown-rot. It is a common fungus in Hawaii (Hemmes and Desjardin 2002) and is frequently associated with plywood, 2 by 4s, lanai railings, or any other wood that is wet. The other fungi could not be definitively identified to species because of the lack of basidiospores in the dried samples. The red fruiting bodies in Figures 4a and 5a are tentatively identified as the polypore *Pycnoporus sanguineus,* a white-rot fungus that is one of the most common shelf polypores in Hawaii (Hemmes and Desjardin 2002), where it is commonly found on stumps and fallen logs and branches. The green fruiting body shown in Figure 5a is most likely a species of the genus *Chlorociboria,* a staining fungus that does not cause significant decay. Other fungi shown in Figures 4b and 5b may include species within the white-rot genera *Phellinus* and possibly *Ganoderma*; identification to species was not possible owing to the extensive degeneration of the old fruiting bodies. Several small, thin fruiting bodies were also observed; these were sterile and could not be identified to genus. The material supports a wide variety of wood-inhabiting fungi, many of which can cause decay.

Density loss

Table 2 shows density measurements obtained on both reference and exposed samples. The reference sample and the exposed shadow and sun samples collected in 2009 all had densities of about 0.92 g/cm^3. Based on these density measurements, the exposed samples collected in 2009 appear to have undergone no decay at the time they were collected. In contrast, the exposed shadow and sun samples collected in 2012 had average densities of 0.65 g/cm^3 and 0.80 g/cm^3, respectively. Compared with the reference sample, this can be calculated as an approximate 51 percent density loss in wood for the shadow-exposed sample and 23 percent density loss in wood for the sun-exposed sample. This density loss indicated that severe decay had occurred between 4.5 and 8 years of exposure. Some variation in density was observed for the exposed boards collected in 2012, particularly for the samples exposed to sun.

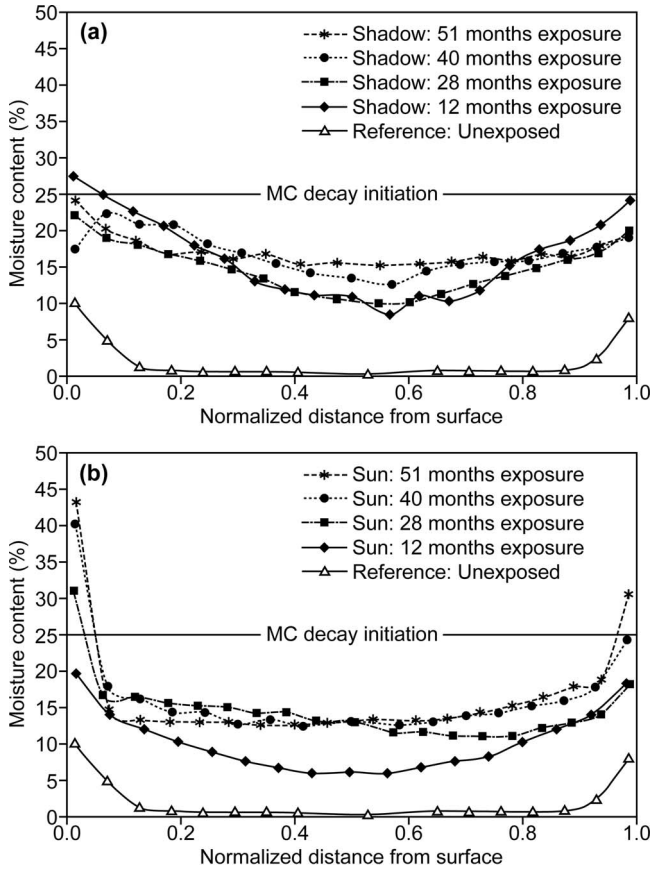

Figure 6.—Moisture content and distribution of (a) shadow and (b) sun boards during their first 51 months of exposure near Hilo, Hawaii.

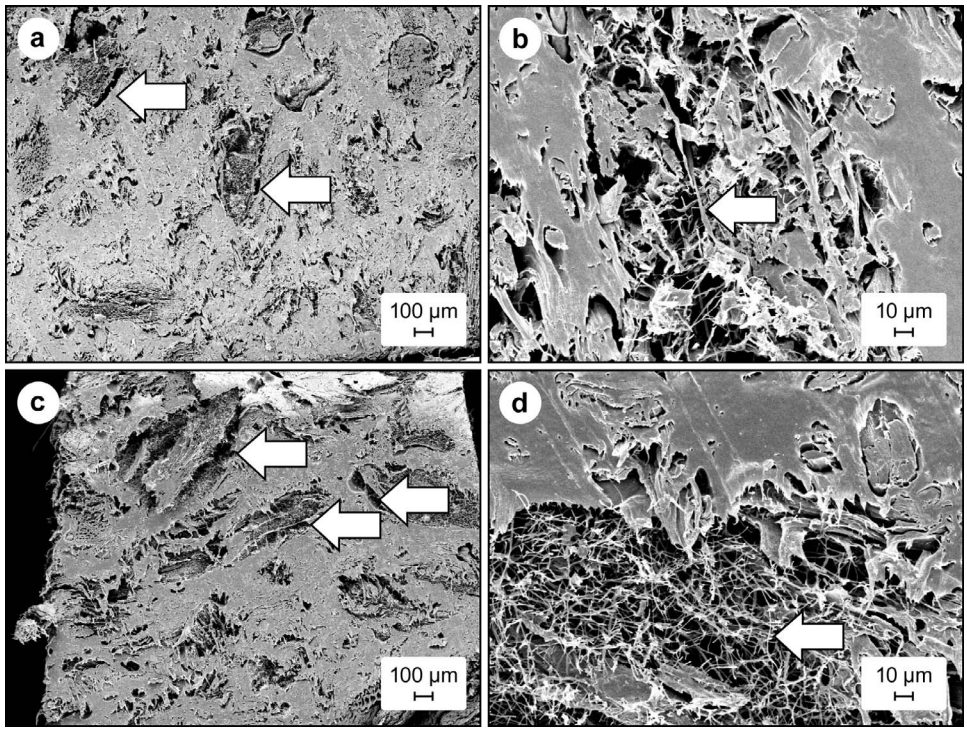

Figure 7.—(a) Scanning electron microscopy (SEM) image taken from Location 5 of the sun sample collected in 2012 (ovendried density of 0.67 g/cm^3). Some areas appear intact, whereas other areas contain masses of hyphae (white arrows). (b) Higher magnification near the center of the same sample (ovendried density of 0.67 g/cm^3) showing a wood particle colonized by fungi with evidence of white-rot decay, including breakdown of cell wall integrity, leading to the formation of a small void (white arrow). (c) SEM image of the same sample (ovendried density of 0.67 g/cm^3) showing voids forming around wood particles from degradation caused by white-rot fungi (white arrows). (d) Higher magnification near the center of image (c).

Historical MC distribution

MC and distribution of the WPC boards during the first 51 months of exposure in both shadow and sun locations are shown in Figure 6. MC and distribution in the graphs indicate relatively moderate WA by the boards during this period. The increase of MC in the core of the boards to 15 to 20 percent after 51 months of exposure seemed to approach the equilibrium MC associated with wetting and drying cycles. The MC in wood exceeded 25 percent only in narrow zones near the board surface in both sun and shadow locations. No severe degradation of the WPC board by fungal decay was expected to occur at this time. The lack of significant decay after 51 months was further confirmed by the density measurements described above, which indicated no obvious density loss in the cross-sectional samples during this period of exposure.

Scanning electron microscopy

SEM images revealed significant decay in sun and shadow samples collected in 2012, which had lower ovendried densities (Figs. 7 and 8). Wood cell walls with severe levels of decay could be observed. The sun sample

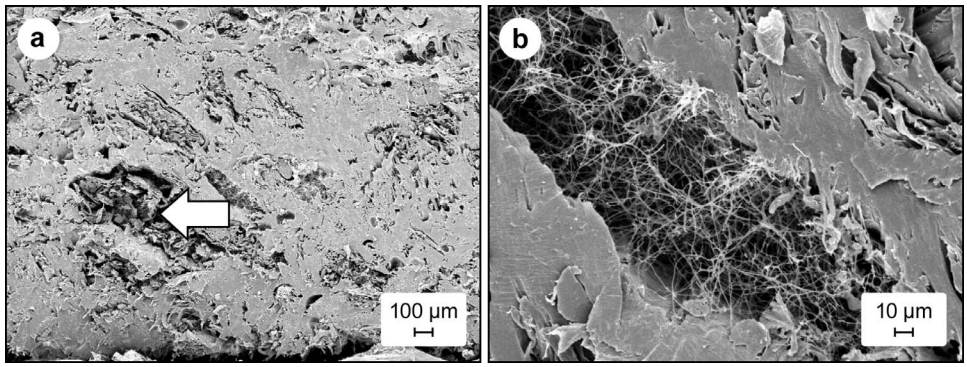

Figure 8.—(a) Scanning electron microscopy (SEM) image of taken from Location 5 of the shadow sample collected in 2012 (ovendried density of 0.60 g/cm^3). Large voids are forming in the sample where wood cell walls have degraded to the point of collapse of structure (white arrow). (b) Higher magnification SEM image near the center of the same sample (ovendried density of 0.60 g/cm^3). Voids have formed where the wood component has been completely degraded, leaving a mass of hyphae occupying the space created.

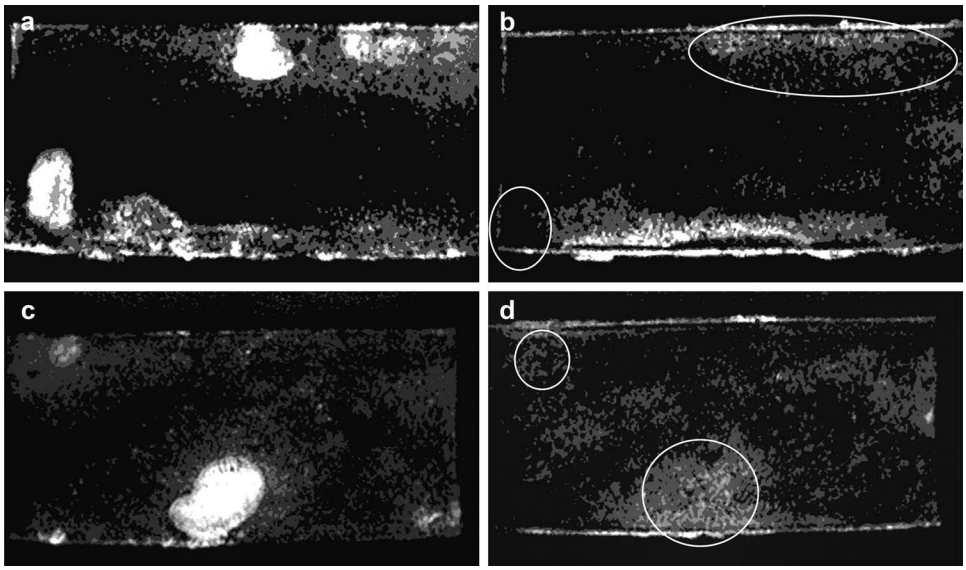

Figure 9.—Magnetic resonance images of the shadow board obtained in Plane 1 at (a) Side A showing the slice at the bottom surface of the board, (b) Side A showing the slice about 8 mm above the bottom surface of the board, (c) Side B showing the slice at the bottom surface of the board, and (d) Side B showing the slice about 8 mm above the bottom surface of the board. Images (a) and (c) mirror the bottom side of the board shown in Figure 4b.

collected in 2012 corresponding to Location 5 (Table 2) and an ovendried density of 0.67 g/cm^3 (Fig. 7) had some relatively sound areas but also areas where masses of fungal hyphae were surrounding the wood particles, causing severe decay resulting in void formation. The 2012 shadow sample at Location 5 (0.60 g/cm^3) had some areas of severe decay (Fig. 8) resulting in voids packed with white-rot fungi (Fig. 8b).

Magnetic resonance imaging

MRI images show significant bright areas (spots) visible at the board surface and at many locations inside the board. In earlier work (Gnatowski et al. 2014), it was shown that light areas indicated the presence of free water in the WPC board at concentrations above the fiber saturation point in the composite voids, including those in wood flour particles.

Board exposed in shadow.—MRI images of the shadow board were obtained in Plane 1 from Sides A and B of the board. Select images representative of the evaluated area are shown in Figure 9. Fungal fruiting bodies, which appear as relatively bright white ovular features, indicating a high concentration of free water, are apparent in images obtained at the very bottom surface of the board. Figure 9a, an image obtained in Plane 1 of the bottom of Side A, shows the presence of free water associated with three fungal fruiting bodies, which were previously seen in Figure 4b. In the same area, another image obtained in the same plane 4 mm above the bottom surface of the board shows that in the vicinity of two of the three fungal fruiting bodies, there is an increase in localized moisture, as indicated by gray regions along the top edge of the image (Fig. 9b). However, there is an obvious lack of free water in the bottom left corner of the image, in an area directly adjacent to the third fungal fruiting body. Figure 9c shows an image obtained in Plane 1 of the bottom of Side B of the board, again displaying the moisture-abundant fruiting bodies present. An MRI slice obtained 4 mm above this area indicates the significant presence of free water throughout the greater portion of the

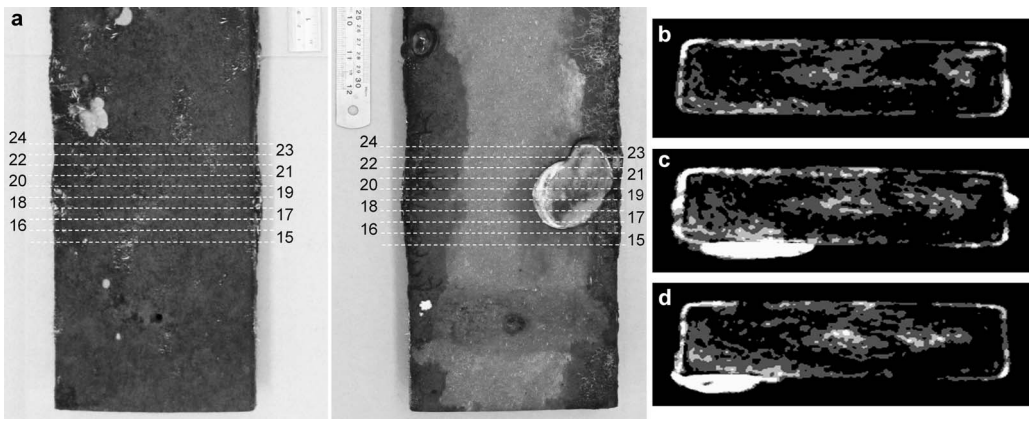

Figure 10.—Images of the shadow board at Side B of the board in the vicinity of a fungal fruiting body showing the location of the slices (a) and magnetic resonance images obtained in Plane 2 of (b) Slice 15, (c) Slice 19, and (d) Slice 23.

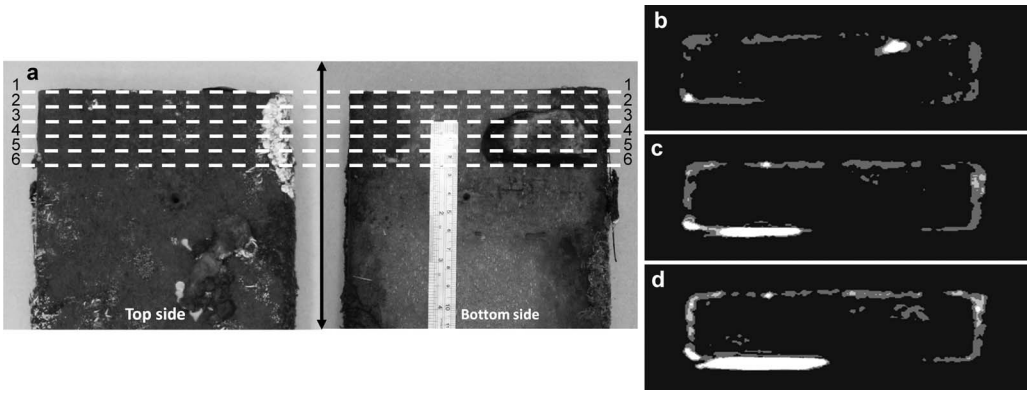

Figure 11.—Images of the shadow board at Side A of the board in the vicinity of a fungal fruiting body showing the location of the slices (a) and magnetic resonance images obtained in Plane 2 of (b) Slice 2, (c) Slice 3, and (d) Slice 4. It should be noted that the bottom side image shown was obtained by flipping the board along the longitudinal axis indicated by the black arrowed line in (a).

imaged area, and in particular, at both locations immediately adjacent to fungal fruiting bodies (Fig. 9d).

Cross-sectional MRI images were obtained in Plane 2 at the location of various fungal fruiting bodies. Figure 10 shows a fruiting body at Side B of the shadow board along with accompanying images obtained in this area. Figure 10b first shows a cross-sectional slice obtained in Plane 2 just to the right of the fruiting body, with low to moderate moisture above the fiber saturation point present at the bottom left corner of the slice. In contrast, Figures 10c and 10d display significantly higher MC in the same area now directly adjacent to a fungal fruiting body, indicated by the bright white feature. In all three images, a significant amount of free water is visible in the core of the samples.

It was found that not all instances of fungal fruiting body presence were accompanied by an increase of localized MC in the area. Cross-section images obtained in the vicinity of a fungal fruiting body at Side A of the shadow board showed little to no free water in the WPC board directly adjacent to the fruiting body, which appears as a bright white feature at the bottom left of the image (Fig. 11).

The images seemed to indicate that although the presence of fungal fruiting bodies was often accompanied by an increase in localized MC in their vicinity, this is not always the case. Zones of high MC could be seen in the images in areas away from fungal fruiting bodies and even frequently in the very core of the WPC board segments, with a lack of free water between the wet core and the board surface. This suggests that decay could very likely occur in areas without the manifestation of fruiting bodies.

Although some cross-section images of the exposed boards seem to indicate very little moisture within the board with only a gray border of moisture along the board surfaces (Figs. 11b through 11d), there were many other cases where a significant amount of water was detected at the core of the samples. Figure 12 shows an image obtained in Plane 2 of the shadow board at Side B, approximately 192 mm from the edge (Slice 7). Aside from a thin moisture-rich border around the surface of the sample, the moisture gradient in this board segment appears to be from within the core of the board to the outside. The pattern and geometry of areas containing free water are very variable in this board segment and are difficult to explain based on the expected mechanism of diffusion related to mass transfer from the exterior environment. This suggests that water generated by the decay process likely plays a significant role in the moisture distribution observed, as discussed later in this section.

A similar pattern of free moisture distribution was also observed in images obtained in Plane 3 of the shadow board segment from both Side A and Side B (Figs. 13 and 14). In both images, a clear moisture-rich layer surrounding the surface of the samples is apparent, as is a significant reverse moisture gradient originating from the core of the cross section.

Board segment exposed in sun.—MRI images of the sun board were obtained in Plane 1 from Side A of the board corresponding to Figure 5b. Fungal fruiting bodies present at the bottom of the board can clearly be seen in the images as brighter areas (Fig. 15a). As could be expected, the fungal fruiting bodies contain a relatively large quantity of free water and are easily identified in the images. An image obtained 4 mm above the bottom surface of the board also showed the concentration of free water, in the form of gray

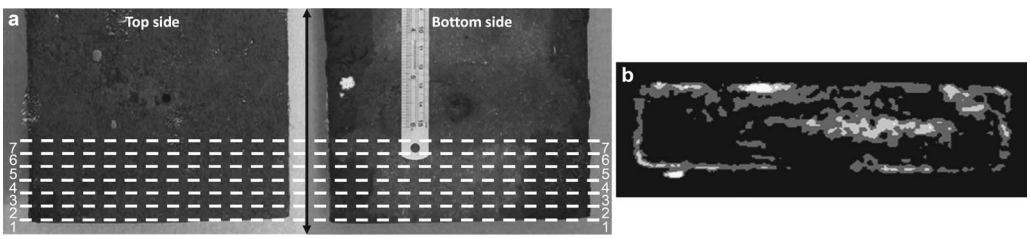

Figure 12.—Images of the shadow board at Side B of the board showing (a) the location of the slices and (b) magnetic resonance image obtained in Plane 2 of Slice 7. It should be noted that the bottom side image shown was obtained by flipping the board along the longitudinal axis indicated by the black arrowed line in (a).

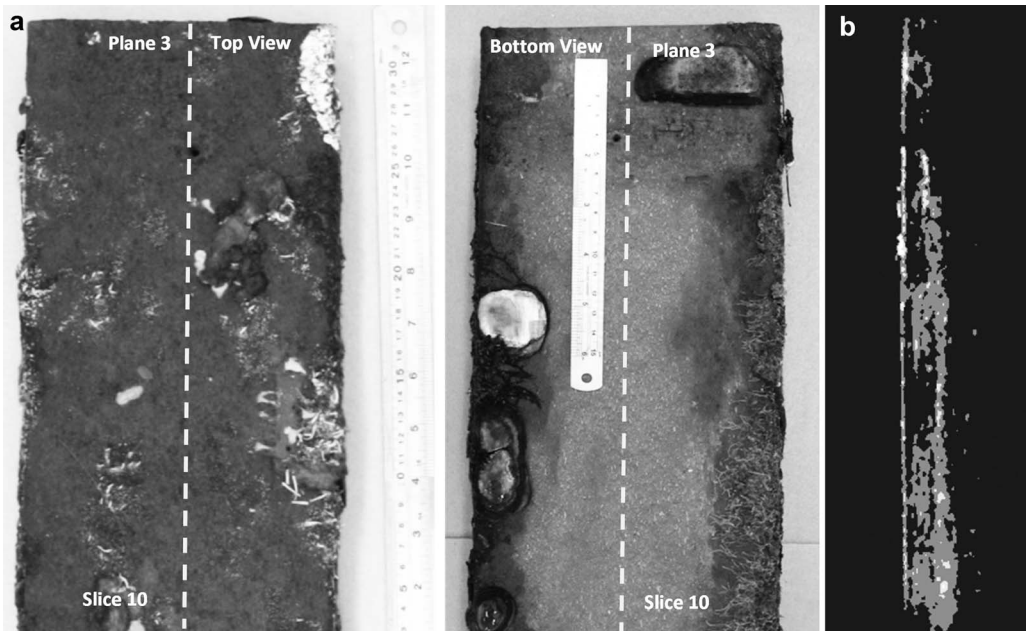

Figure 13.—Images of the shadow board at Side A of the board showing (a) location of the slice and (b) magnetic resonance image obtained in Plane 3 of Slice 10.

areas, in the vicinity of where the fungal fruiting bodies were located (Fig. 15b).

For the board segment exposed in sun, images of the sample cross sections often appeared without the typical light-colored border, indicating a high MC near the surface but a relatively high free water concentration in their core. Figure 16 shows an example of this phenomenon where an image was obtained in Plane 2 of the sun board at Side B, approximately 32 mm from the edge of the board (Slice 4). Another example of this phenomenon can be observed in Figure 17, which shows an image obtained in Plane 3, Side A of the same board, approximately 32 mm from the longitudinal edge on the left-hand side based on the top view of the board. There appears to be a lack of a thin moisture-rich layer at the outer exposed surface of the sample, which is on the left-hand side of the image.

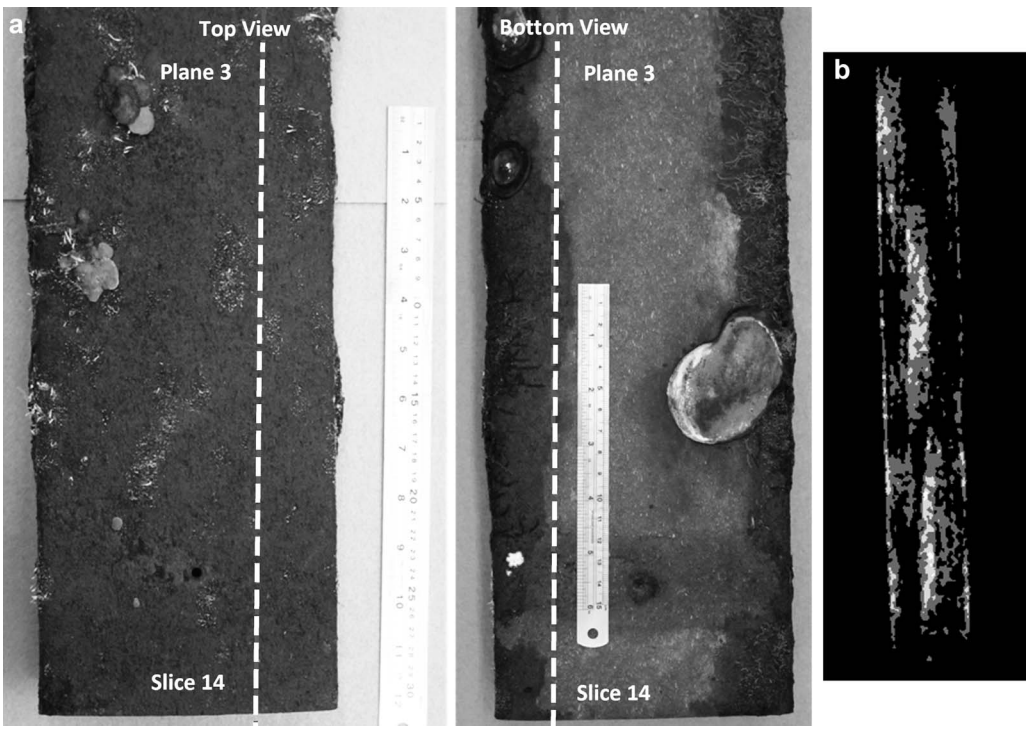

Figure 14.—Images of the shadow board at Side B of the board showing (a) location of the slice and (b) magnetic resonance image obtained in Plane 3 of Slice 14.

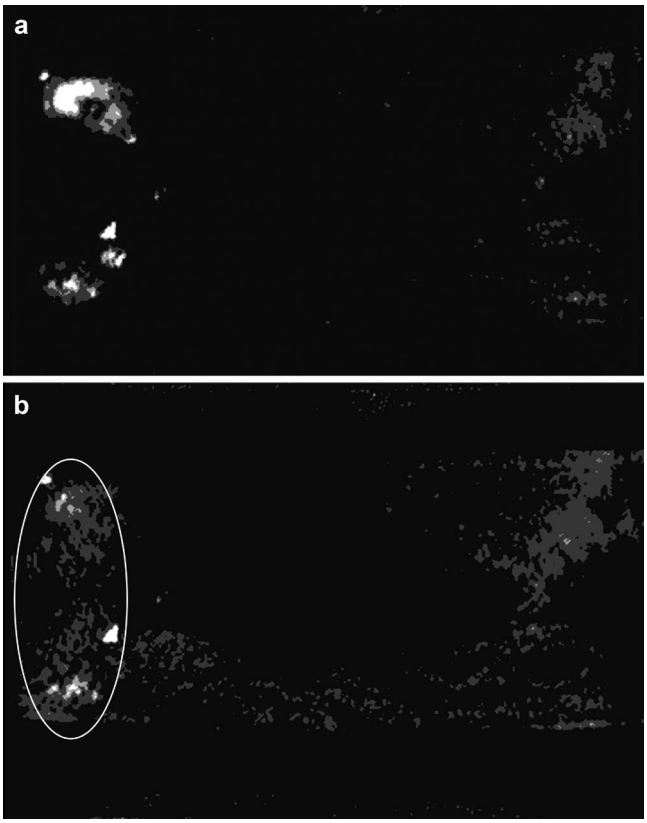

Figure 15.—Magnetic resonance images of the sun board obtained in Plane 1 at Side A showing (a) the slice at the bottom surface of the board and (b) the slice 4 mm above the bottom surface of the board. These images mirror the image of the bottom side of the board shown in Figure 5b.

However, there is an apparent concentration of free water inside the sample near the top of the image (Fig. 17b). This moisture distribution pattern was similarly observed in a Plane 3 cross section from Side B of this sun board segment, obtained approximately 56 mm from the longitudinal edge of the board (Fig. 18). Again, there is clearly a moisture-rich layer at the exposed surface of the board; however, there appears to be a thin zone of high free water content in the core of the sample.

The sun- and shadow-exposed board segments were located less than 3 km apart at the exposure sites near Hilo, Hawaii, and samples were collected on the same day. It is therefore interesting to note the lack of a moisture-rich border for the sun-exposed samples compared with their shadow-exposed counterparts. One possible explanation for this phenomenon is the fact that the MC near the external part of the board, such as the region bordering the board surface, is very sensitive to drying and wetting cycles. This could be particularly true for samples exposed in the sun and may be the reason why a moisture-rich boundary was not observed in these samples.

As mentioned, the MC consisting of free water was found to be above the wood fiber saturation point, indicating that favorable conditions were present for the initiation of decay. Regarding the mechanism of decay, it could be expected that initially there was diffusion of water from the outside to the inside of the WPC. In certain areas, water migration may have been faster, such as in the board support area or in regions promoted by the presence of composite defects or an increased number of microcracks that developed. An example of a composite defect in the form of recycled plastic contamination in the vicinity of a fungal decay fruiting body is shown in Figure 3 for the sun board. This moisture entering the interior of the WPC board segments played a role in triggering localized fungal growth. However, it can be seen in these MRI images that there is a significant amount of water in the interior of the boards and that aside from a thin layer of water around the board surface for some samples, such as those exposed in shadow, there appears to be a reverse moisture gradient from the center of the board to the outside. The relatively slow moisture diffusion within WPC is well documented in literature (Griffin 1977, Müller et al. 2001, Wang and Morrell 2004), and it is reasonable to expect that once initiated, fungal growth will generate additional quantities of water during wood digestion, through the release of free water that would have been bonded to degraded fibers. This water may have difficulty diffusing out from WPC board interior. The accumulation of water inside a WPC board will create more favorable conditions for fungal growth at the WPC subsurface, which at some point may become self-propagating. This mechanism of moisture generation inside WPC boards associated with the board decay process explains the reverse moisture gradient observed as well as rapid fungal decay occurring after an initiation period.

Some comments should also be made regarding the absence of free water as detected by MRI. For the sun board, individual samples that showed a lower density (Table 2, Locations 4 through 6) were located in the area of the MRI image (Fig. 16b) that exhibited no free moisture (black region on the right side). In contrast, individual samples with higher density (Table 2, Locations 1 through 3) were located in the zones displaying the presence of free water (lighter gray area on left side). Based on available data, it could be expected that a lack of free moisture in an MRI image could mean decay activity has already progressed significantly, with the majority of wood having been metabolized, as was seen on MRI images for samples collected after 8 years of exposure. There is effectively no

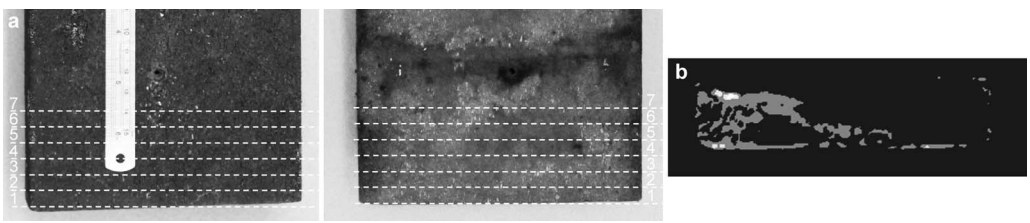

Figure 16.—Images of the sun board at Side B of the board showing (a) location of the slices and (b) magnetic resonance image obtained in Plane 2 of Slice 4.

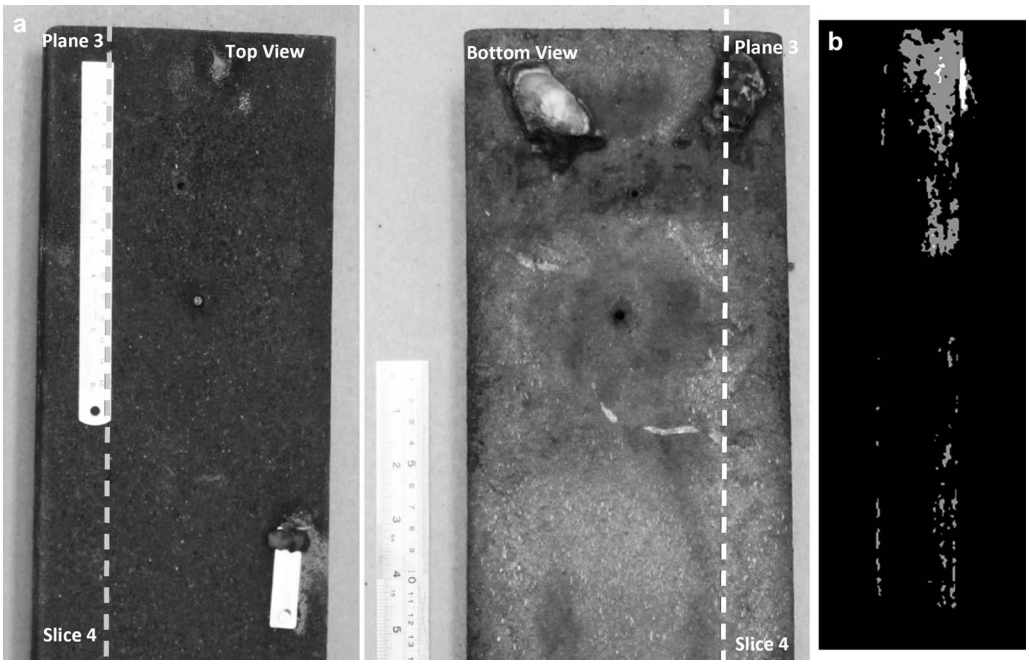

Figure 17.—Images of the sun board at Side A of the board showing (a) location of the slice and (b) magnetic resonance image obtained in Plane 3 of Slice 4.

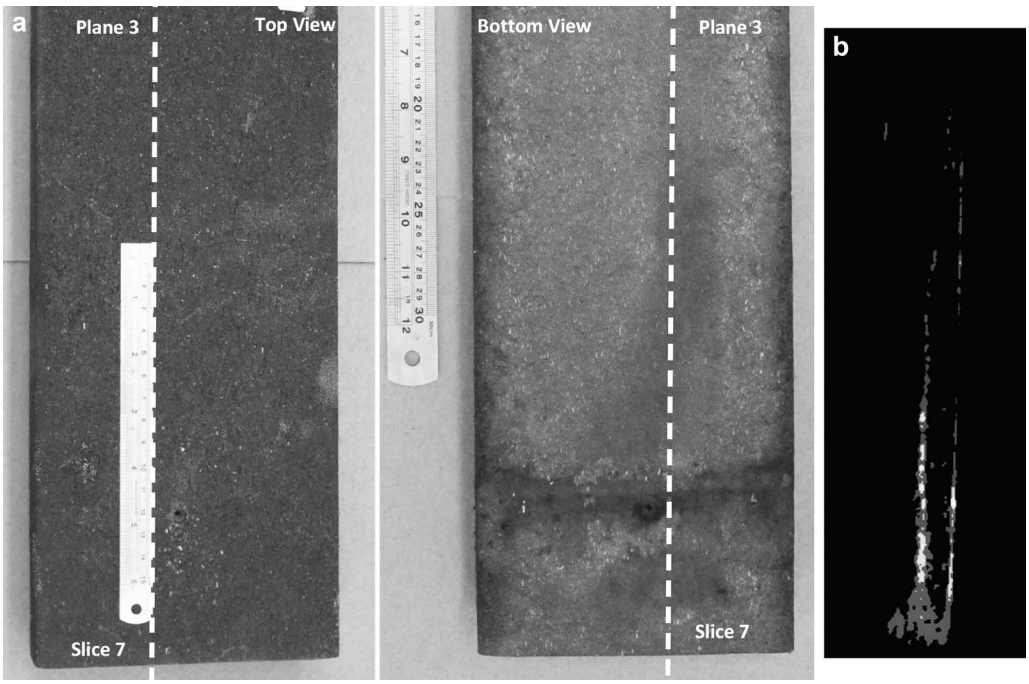

Figure 18.—Images of the sun board at Side B of the board showing (a) location of the slice and (b) magnetic resonance image obtained in Plane 3 of Slice 7.

wood left to harbor the moisture, and the remaining moisture has already diffused out of this area. This observation was confirmed by the density measurements and SEM images of the samples, which indicated advanced and severe decay.

Conclusions

Severe fungal decay activity in field-exposed WPC boards that exhibited a significant decrease in density was confirmed by SEM, where masses of fungal hyphae causing cell wall destruction could be observed. MRI was used to detect MC and distribution above the wood fiber saturation point in these decaying WPC boards. Contrary to historical moisture distribution data for WPCs with little or no decay, which showed free water accumulation only within a few millimeters of the surface, MRI of the decayed WPCs indicated a significant amount of water distributed randomly all across the board cross sections, including the core of the samples. In previously examined exterior-exposed boards

that had yet to show symptoms of decay, the pattern of free water distribution had appeared to be exclusively a moisture gradient from the outside of the board inward. In the decayed WPCs examined in this investigation, the opposite was found in many places, where a reverse moisture gradient could be observed from the core of the boards to the outside. This could be reasonably explained by both the transport of moisture by fungal mycelia to a particular area of activity and by the generation of water as decay fungi metabolize wood, releasing bound water. Combined with the low water permeability inherent to WPCs, this would likely increase the internal MC of the boards, accelerate decay, and create a self-propagating decay process once it is initiated. This may also explain the decay initiation period during which little or no decay is observed, followed by a significantly accelerated decay process later in the exposure.

Fungal fruiting bodies, which are an indication of aggressive decay, did not appear to be consistently associated with high MC in the surrounding area. Many of these fruiting bodies were old, and their associated mycelia may no longer be actively decaying wood particles. The presence of fungal fruiting bodies may not be the only indicator of decay, as zones of high free water concentration were readily observed throughout many other areas of the evaluated boards. The presence of high MC inside WPC boards with only limited moisture present near the surface is difficult to explain by phenomena other than an active decay process.

Acknowledgments

The authors thank Irene Kinoshita of Canadian Magnetic Imaging Laboratory for her assistance, advice, and MRI work on the WPC boards, and Karen Nelson from the Forest Products Laboratory for her assistance with the figures.

Literature Cited

ASTM International. 2014a. Standard test methods for evaluating properties of wood-base fiber and particle panel materials. ASTM Standard D1037-12. ASTM International, West Conshohocken, Pennsylvania. 31 pp.

ASTM International. 2014b. Standard guide for evaluating mechanical and physical properties of wood-plastic composite products. ASTM Standard D7031-11. ASTM International, West Conshohocken, Pennsylvania. 8 pp.

Bucur, V. 2003. Nuclear magnetic resonance. *In:* Nondestructive Characterization and Imaging of Wood. Springer-Verlag, Berlin. pp. 215–279.

Clemons, C. M. and R. E. Ibach. 2002. Laboratory tests on fungal resistance of wood filled polyethylene composites. *In*: Proceedings of ANTEC, May 5–9, 2002, San Francisco; Society of Plastics Engineers, Newtown, Connecticut. pp. 2219–2222.

Defoirdt, N., S. Gardin, J. Van den Bulcke, and J. Van Acker. 2010. Moisture dynamics of WPC and the impact on fungal testing. *Int. Biodeterior. Biodegrad*. 64:65–72.

Fabiyi, J. S., A. G. McDonald, J. J. Morrell, and C. Freitag. 2011. Effects of wood species on durability and chemical changes of fungal decayed wood plastic composites. *Compos. Part A Appl. Sci. Manuf*. 42:501–510.

Gilbertson, R. L. and L. Ryvarden. 1986. North American Polypores. Vol. 1. Fungiflora, Oslo. pp. 1–433.

Gilbertson, R. L. and L. Ryvarden. 1987. North American Polypores. Vol. 2. Fungiflora, Oslo. pp. 434–885.

Gnatowski, M., R. E. Ibach, M. Leung, and G. Sun. 2014. Magnetic resonance imaging used for the evaluation of water presence in wood plastic composite boards exposed to exterior conditions. *Wood Mater. Sci. Eng*. 10(1):94–111.

Griffin, D. M. 1977. Water potential and wood-decay fungi. *Ann. Rev. Phytopathol*. 15:319–329.

Hall, L. D., V. Rajanayagam, W. A. Stewart, and P. R. Steiner. 1986. Magnetic resonance imaging of wood. *Can J. Forest Res*. 16(2):423–426.

Hanawalt, K. 2012. Wood-plastic composites done right. Plastics technology. www.ptonline.com/articles/wood-plastics-composites-done-right. Accessed May 27, 2015.

Hemmes, D. E. and D. E. Desjardin. 2002. Mushrooms of Hawai'i. Ten Speed Press, Berkeley, California. 212 pp.

Ibach, R. E. and C. Clemons. 2002. Biological resistance of polyethylene composites made with chemically modified fibre or flour. *In:* Sixth Pacific Rim Bio-Based Composites Symposium, P. E. Humphrey (Ed.), Oregon State University, Portland. pp. 574–583.

Ibach, R. E., C. Clemons, and N. M. Stark. 2004. Combined ultraviolet and water exposure as a preconditioning method in laboratory fungal durability testing. *In:* Seventh International Conference on Woodfiber–Plastic Composites, N. Stark (Ed.), May 19–20, 2003, Madison, Wisconsin; Forest Products Society, Madison, Wisconsin. pp. 61–67.

Ibach, R. E., M. Gnatowski, and G. Sun. 2013. Field and laboratory decay evaluations of wood-plastic composites. *Forest Prod. J*. 63(3/4):76–87.

Jin, X., R. G. M. van der Sman, E. Gerkema, F. J. Vergeldt, H. van As, and A. J. B. van Boxtel. 2011. Moisture distribution in broccoli: Measurements by MRI hot air drying experiments. *In:* 11th International Congress on Engineering and Food (ICEF11). SciVerse ScienceDirect. *Procedia Food Sci*. 1:640–646.

Jones, M., P. S. Aptaker, J. Cox, B. A. Gardiner, and P. J. McDonald. 2012. A transportable magnetic resonance imaging system for in situ measurements of living trees. The Tree Hugger. *J. Magnetic Res*. 218:133–140.

Kim, J. W., D. P. Harper, and A. M. Taylor. 2008. Effect of wood species on water sorption and durability of wood–plastic composites. *Wood Fiber Sci*. 40:519–531.

Kim, J. W., D. P. Harper, and A. M. Taylor. 2009. Effect of extractives on water sorption and durability of wood–plastic composites. *Wood Fiber Sci*. 41:279–290.

Kirk, T. K. and E. B. Cowling. 1984. Biological decomposition of solid wood. *In:* The Chemistry of Solid Wood. R. Rowell (Ed.). American Chemical Society, Washington, D.C. pp. 455–487.

Klyosov, A. A. 2007. Wood-Plastic Composites. John Wiley & Sons, Hoboken, New Jersey. 105 pp.

Laks, P. E., D. L. Richter, G. M. Larkin, and J. O. Eskola. 2010. A survey of the biological resistance of commercial WPC decking. *In*: Tenth Pacific Rim Bio-Based Composites Symposium, October 5–8, 2010, Banff, Alberta, Canada. pp. 193–201.

Laks, P. E. and S. A. Verhey. 2000. Decay and termite resistance of thermoplastic/wood fibre composites. *In:* Proceedings of the 5th Pacific Rim Bio-Based Composites Symposium, P. D. Evans (Ed.), December 10–13, 2000, Canberra, Australia; Department of Forestry, Australian National University, Canberra, Australia. pp. 727–734.

Lomelí-Ramírez, M. G., H. G. Ochoa-Ruiz, F. J. Fuentes-Talavera, S. García-Enriquez, M. A. Cerpa-Gallegos, and J. A. Silva-Guzmán. 2009. Evaluation of accelerated decay of wood plastic composites by Xylophagus fungi. *Int. Biodeterior. Biodegrad*. 63:1030–1035.

Lopez, J. L., P. A. Cooper, and M. Sain, 2005. Evaluation of proposed test methods to determine decay resistance of natural fiber plastic composites. *Forest Prod. J*. 55:95–99.

MacMillan, B., E. Veliyulin, C. Lamason, and B. J. Balcom. 2011. Quantitative magnetic resonance measurements of low moisture content wood. *Can. J. Forest Res*. 41:2158–2162.

Mankowski, M. and J. J. Morrell. 2000. Patterns of fungal attack in wood–plastic composites following exposure in a soil block test. *Wood Fiber Sci*. 32:340–345.

Manning, M. J. and F. Ascherl. 2007. Wood–plastic composite durability and the compelling case for field testing. *In:* Ninth International Conference on Wood and Biofiber–Plastic Composites, May 21–23, 2007, Madison, Wisconsin; Forest Products Society, Madison, Wisconsin. pp. 217–224.

Morris, P. I. and P. Cooper. 1998. Recycled plastic/wood composite lumber attacked by fungi. *Forest Prod. J*. 48:86–88.

Müller, U., R. Bammer, E. Halmschlager, R. Stollberger, and R. Wimmer. 2001. Detection of fungal wood decay using magnetic resonance imaging. *Holz Roh- Werkst*. 59:190–194.

Naghipour, B. 1996. Effects of extreme environmental conditions and fungal exposure on the properties of wood–plastic composites. Master's thesis. University of Toronto, Toronto. 70 pp.

Olson, J. R. and S. J. Chang. 1990. Nuclear magnetic resonance imaging: A non-invasive analysis of moisture distributions in white oak lumber. *Can. J. Forest Res*. 20:586–591.

Pendleton, D. E., T. A. Hoffard, T. Adcock, B. Woodward, and M. P. Wolcott. 2002. Durability of an extruded HDPE/wood composite. *Forest Prod. J*. 52:21–27.

Schauwecker, C., J. J. Morrell, A. G. McDonald, and J. S. Fabiyi. 2006. Degradation of a wood-plastic composite exposed under tropical conditions. *Forest Prod. J*. 56:123–129.

Segerholm, B. K., R. W. Ibach, and M. E. P. Walinder. 2012. Moisture sorption in artificially aged wood–plastic composites. *Bioresources* 7:1283–1293.

Shirp, A. and M. P. Wolcott. 2005. Influence of fungal decay and moisture absorption on mechanical properties of extruded wood–plastic composites. *Wood Fiber Sci*. 37:643–652.

Smith, P. M., and M. P. Wolcott. 2006. Opportunities for wood/natural fiber–plastic composites in residential and industrial applications. *Forest Prod. J*. 56:4–11.

Stenstrom, S., C. Bonazzi, and L. Foucat. 2009. Magnetic resonance imaging for determination of moisture profiles and drying curves. *In:* Modern Drying Technology: Experimental Techniques. E. Tsotsas and A. S. Mujumdar (Eds.). Wiley-VCH Verlag GmbH & Co. KGaA, Weinheim, Germany. pp. 91–142.

Telkki, V. V., J. Saunavaara, and J. Jokisaari. 2010. Time-of-flight remote detection MRI of thermally modified wood. *J. Magnetic Res*. 202:78–84.

Verhey, S. A., P. E. Laks, and D. L. Richter. 2001. Laboratory decay resistance of woodfiber/thermoplastic composites. *Forest Prod. J*. 51:44–49.

Verhey, S. A., P. E. Laks, D. L. Richter, E. D. Keranen, and G. M. Larkin. 2003. Use of field stakes to evaluate the decay resistance of woodfiber–thermoplastic composites. *Forest Prod. J*. 53:67–74.

Wang, P. C. and S. J. Chang. 1986. Nuclear magnetic resonance imaging of wood. *Wood Fiber Sci*. 18(2):308–314.

Wang, W. and J. J. Morrell. 2004. Water sorption characteristics of two wood-plastic composites. *Forest Prod. J*. 54:209–212.